THE VOLT-AMPERE CHARACTERISTICS OF AN MHD GENERATOR WITH A FIXED DIRECTION FOR THE ELECTRIC FIELD AND A SINGLE LOAD

A. I. Él'kin and E. I. Yantovskii

Magnitnaya Gidrodinamika, Vol. 5, No. 3, pp. 74–80, 1969

UDC 538.3:533.95:538.4:621.362

The volt-ampere characteristics of an MHD generator with fixed direction of the electric field is considered in the quasi-one-dimensional approximation; this refers to a frame channel and a single load, in the absence of a longitudinal current in the nominal regime.

Calculations on a Ural-4 computer show that, in addition to the regimes of shockfree flow in an MHD channel (regime I), it is possible to have flows with a compression shock in the channel (regime II) or in a nozzle (regime III). We have constructed the volt-ampere characteristics for each of the possible regimes. We show that the volt-ampere characteristics for regime I is nonlinear, while its slope at the design point increases with an increase in the parameter of MHD interaction. Unlike the flows in tubes with friction, the maximum channel length (corresponding to the speed of sound at the outlet) in the presence of a compression shock in the channel or in the nozzle may be smaller than the maximum length in the case of shockfree flow. The volt-ampere characteristics for regimes I and II can be constructed only for currents greater than some minimum. The shockfree flow involving thermodynamic blockage at the channel outlet corresponds to such a current. For regime III no such limitation exists.

§ 1. The expressions for the specific power and local electrical efficiency coefficient of this type of MHD generator were first derived by Montardi [1]. The operation of this circuit in quasi-one-dimensional approximation was analyzed in [2–4]. In particular, the MHD-generator class with a fixed electric-field direction and a single load is examined in [4] on the assumption that there is no longitudinal current. The specific power assumes the maximum possible value for a fixed electrical efficiency in this case. A number of regimes were analyzed in [4] and it was demonstrated that for polyatomic gases (k < 1, 2) the supersonic flow regime is effective when the equipotentials exhibit a slope (variable) such that there is no longitudinal current in the gas and the local coefficient of electrical efficiency is constant. For this flow regime ($j_x = 0$, $\eta_{el} = \text{const}$) we find that a specific geometry corresponds to a particular value of the theoretical electrical efficiency η_{el}, i.e., we obtain the shape of the channel and the law governing the variation in the slope of the equipotentials over length, in addition to a specific value for the load current I. Having established the channel geometry, it would be interesting to examine the relationship between the generator voltage and its current, i.e., the volt-ampere characteristic. In this case we should evidently maintain the conditions $j_x = 0$ and $\eta_{el} = \text{const}$ in the theoretical (nominal) regime. An analysis of this kind makes it possible to investigate in greater detail the properties of an MHD generator and to determine the additional limitations which could not be established from an analysis of the theoretical regimes alone. The form of the volt-ampere characteristic of an MHD generator is a function of the installation circuit of which the generator is a part. For simplicity we will assume that the parameters of the gas adiabatically stagnated in the receiver, from which the gas enters a Laval nozzle with a fixed geometry and then into the MHD generator, is independent of the loading regime, and that the pressure of the medium at the channel outlet (the counterpressure) is maintained as in the nominal regime.

The system of equations which, in quasi-one-dimensional approximation, describes the flow of a gas in the channel of an ideally segmented MHD generator with a fixed direction for the electric field and a single load is as follows:

$$\rho v\frac{dv}{dx}=-\frac{dp}{dx}+j_yB;\quad \rho v\frac{d}{dx}\left(c_pT+\frac{v^2}{2}\right)=\frac{E_xI}{F};$$

$$j_x=\frac{\sigma[E_x-\beta(E_y-vB)]}{1+\beta^2};\quad j_y=\frac{\sigma(E_y-vB+\beta E_x)}{1+\beta^2};$$

$$p=\rho gRT;\quad \rho vF=G;\quad F(j_x+j_y/\gamma)=I;$$

$$\sigma=\sigma_1\left(\frac{T}{T_1}\right)^{\alpha}\sqrt{\frac{p_1}{p}};\quad \beta=\beta_1\frac{\rho_1}{\rho}\sqrt{\frac{T_1}{T}}. \qquad (1)$$

Here γ is the slope of the frame. We introduce the following dimensionless quantities:

$$\bar{v}=v/v_{01};\quad \tau=T/T_{01};\quad \bar{F}=F/F_1;\quad \bar{x}=x/L;$$

$$S=\sigma_{01}B^2L/\rho_{01}v_{01};\quad \tilde{I}=I/\sigma_{01}v_{01}B_{01}F_{01};$$

$$\tilde{u}=B\sigma_{01}u/\rho_{01}v_{01}^2;\quad k=c_p/c_v;$$

$$a=2[(k-1)^{-1}-\eta_{el0}(2\alpha+1)k^{-1}](\eta_{el0}-1)^{-1}M_1^{-2};$$

$$c=[(k-1)^{-1}-2\alpha](\eta_{el0}-1)^{-2}M_{01}^{-2}k^{-1}S^{-1};\quad \tilde{\bar{u}}=\tilde{u}/\tilde{u}_0;$$

$$\tilde{\bar{I}}=\tilde{I}/\tilde{I}_0;\quad \tilde{a}=1-\tau/\bar{v}^2kM_{01}^2;$$

$$\tilde{d}=\bar{v}^{-1}(k-1)^{-1}M_{01}^{-2};\quad \tilde{b}=(\bar{v}kM_{01})^{-1};$$

$$\tilde{c}=\frac{S\tau^{\alpha-1/2}\bar{F}^{1/2}\bar{v}^{1/2}}{1+\beta^2}(k_y-1+\beta\gamma)+\tau\frac{d\bar{F}}{d\bar{x}}(\bar{F}\bar{v}kM_{01}^2)^{-1};$$

$$k_y=E_y/vB=[1+\gamma(1+\beta^2)\bar{I}\tau^{1/2-\alpha}\bar{F}^{-1/2}\bar{v}^{-3/2}-\beta\gamma](\gamma^2+1)^{-1}.$$

Here subscript 1 corresponds to the generator inlet parameters, while subscript zero corresponds to the parameters in the nominal regime for which, when $j_x = 0$ and $\eta_{el} = \text{const}$, system (1) is integrated in quadratures [4].

Those formulas pertaining to the nominal regime which we will require later on are:

$$\bar{F}=\bar{F}_0=\bar{v}_{01}^{-1}\tau_0^{-2\alpha}; \qquad (2)$$

$$\gamma=\gamma_0=(\eta_{el0}-1)\eta_{el0}^{-1}\beta_1\bar{v}_0\bar{F}\tau_0^{-1/2}; \quad (3)$$

$$\frac{d\bar{F}}{d\bar{x}}=-\frac{\bar{v}_0}{c\tau_0^{2\alpha+1/2}}(2a\bar{v}_0^{-3}\tau_0^{-2\alpha}+2\alpha\bar{v}_0^{-1}\tau_0^{-1-2\alpha}); \quad (4)$$

$$\bar{v}_0=\sqrt{a(\tau_0-1)+1}; \quad (5)$$

$$\frac{d\tau_0}{d\bar{x}}=\bar{v}_0\tau_0^{-2\alpha-1/2}c^{-1}. \quad (6)$$

We rewrite system (1) as

$$\frac{d\bar{v}}{d\bar{x}}=(\tilde{c}\tilde{d}-\tilde{I}\gamma S k_y\tilde{b})(\tilde{a}\tilde{d}-\tilde{b}); \quad (7)$$

$$\frac{d\tau}{d\bar{x}}(\tilde{a}\gamma\tilde{I}Sk_y-\tilde{c})(\tilde{a}\tilde{d}-\tilde{b}). \quad (8)$$

The parameter S can be treated as the dimensionless length of the channel.

$$\tilde{U}=\frac{\bar{v}^2-1}{2\tilde{I}}+\frac{\tau-1}{\tilde{I}M_{01}^2(k-1)}. \quad (9)$$

Having integrated system (6)–(8) for various values of the current $\tilde{I}$ and having calculated the voltage from formula (9), we find the desired volt-ampere characteristic. Here the geometry is assumed to be specified by formulas (2)–(4). The right-hand members of these formulas are functions of the parameter τ_0—the dimensionless temperature in the theoretical regime, which in turn is a function of the longitudinal coordinate, according to (6). Since (6) is not integrated, it is advisable to combine (6) with (7) and (8) and to solve the resulting system simultaneously. Of course, for the theoretical current $\tilde{I}=\eta_{el0}/\beta_{01}$ we must maintain the condition $\tau=\tau_0$. If this nozzle is operating in the theoretical regime, the initial conditions for the integration of (6)–(8) are

$$\bar{v}_1=\tau_1=\tau_{01}=1. \quad (10)$$

§ 2. The system of equations (6)–(9) with initial conditions (10) was integrated by the Runge-Kutta method on a Ural-4 computer. The corresponding volt-ampere characteristics for $M_{01}=2.2$, $\beta_{01}=5$, $k=1.115$, and various values of the MHD interaction parameter S are shown in Fig. 1. The characteristics are nonlinear—convex when $\bar{I}<1$ and concave when $\bar{I}>1$. With a change in the current $\bar{I}$ from the nominal value $\bar{I}=1$ to a standing current $\bar{I}=0$, the flow regime in the MHD channel changes (Fig. 2a). With a reduction in the current $\bar{I}$, the Mach number M over the channel length (we have taken the MHD interaction parameter S as the dimensionless length) begins to drop off sharply, until thermodynamic blockage occurs (Fig. 2a) at some current $\bar{I}_\alpha$. This means that the possibility of continuous flow exists only for currents greater than some specific value. Accordingly, the volt-ampere characteristics in Fig. 1, for regimes in which shockfree variations in the thermodynamic parameters over the length of the channel occur, can be constructed in the region from the short-circuit current to some current $\bar{I}_\alpha<1$, corresponding to the regime of thermodynamic blockage. It should be noted that for any value of the current, as demonstrated by calculation, the following condition is maintained:

$$p>p''. \quad (11)$$

Here p is the pressure at the outlet from the channel of the MHD generator, while the pressure p" is associated with the counterpressure p' of the medium by the relationship for the normal compression shock [6]:

$$p''=p'[1+2k(k+1)^{-1}(M^2-1)]^{-1}. \quad (12)$$

From this we can apparently draw the conclusion, in analogy with nozzle flow ([5], p. 153), that it is impossible in this case to have MHD flow with a compression shock in the MHD channel, nor subsequently to restore the pressure to the pressure of the medium when the conditions at the outlet are subsonic.

The slope of the volt-ampere characteristic $d\bar{U}/d\bar{I}$ at the calculation point is the limit of the numerical sequence

$$\frac{\bar{U}(\bar{I}=1+\delta)-\bar{U}(\bar{I}=1)}{\delta},$$

$$\frac{\bar{U}(\bar{I}=1+2^{-1}\delta)-\bar{U}(\bar{I}=1)}{2^{-1}\delta},\ldots,$$

$$\frac{\bar{U}(\bar{I}=1+2^{1-n}\delta)-\bar{U}(\bar{I}=1)}{2^{1-n}\delta},\ldots.$$

Figure 3 shows the slope as a function of the parameter S.

The quantity $d\bar{U}/d\bar{I}$ increases sharply as S increases and for large values of S it may be larger by one or two orders of magnitude than when S = 0, i.e., in the calculation of the volt-ampere characteristic assuming uniform parameter distribution. When S = 0, using the expression for the load current I, Ohm's law (1), and the additional condition $\gamma=(\eta_{el}-1)\eta_{el}^{-1}\beta$, following from (3) when S = 0, we obtain the following expression for $d\bar{U}/d\bar{I}$:

$$\frac{d\bar{U}}{d\bar{I}_{S=0}}=\frac{\beta^{-1}+\beta}{\beta^{-1}(1-\eta_{el}^{-1})^{-1}+\beta(1-\eta_{el}^{-1})}. \quad (13)$$

The numerical values of $d\bar{U}/d\bar{I}$, calculated according to (13), coincide with the values obtained in the integration of the system of equations (6)–(8) as $S\to 0$, as was to be expected.

§ 3a. Earlier we examined flow regimes with a continuous variation in parameters over channel length. Let us now consider the possibility of the existence of flow regimes with a normal compression shock in the MHD channel or in the nozzle. As before, system (6)–(8) is valid within the entire region; however, in the section in which we assume the existence of the compression shock the quantities $\bar{v}$ and τ undergo a discontinuity which is defined [6] by the relationship on the shock:

$$\tau'/\tau''=2(k-1)(k+1)^{-2}(M')^{-2}\times$$

$$\times[2kM'(k-1)^{-1}-1][1+{}^1/_2(k-1)(M')^2];$$

$$\bar{v}'/\bar{v}''=[1+(k-1)/2\cdot(M')^2\cdot 2(k+1)^{-1}(M')^{-2}. \quad (14)$$

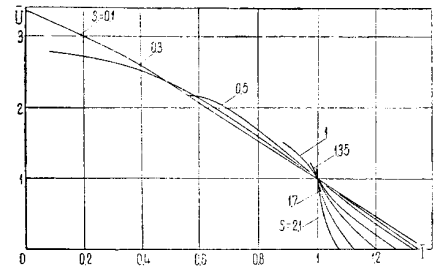

Fig. 1. Volt-ampere characteristics in regime I.

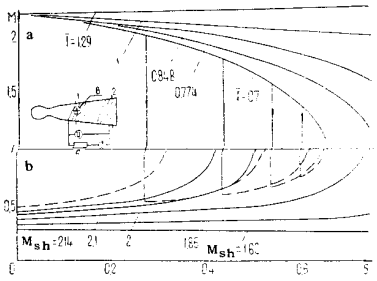

Fig. 2. Variation in the Mach number over channel length: a) for shock-free flow at various currents; b) for flow regimes with a shock in the MHD channel (dashed curves) and in the nozzle (solid curves) at a current of $\bar{I}$ = 0.7 and for various locations of the shock.

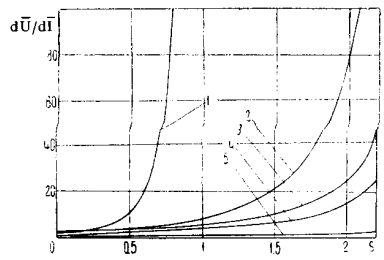

Fig. 3. Slope of the voltage ampere characteristic of regime I as a function of the MHD interaction parameter: 1) β_1 = 5; η_{el1} = 0.7; k = 1.15; 2) β_1 = 5; η_{el1} = 0.85; k = 1.15; 3) β_1 = = 5; η_{el1} = 0.85; k = 1.115; 4) β_1 = 3.75, η_{el1} = 0.85; k = 1.14; 5) β_1 = 2.5; η_{el1} = = 0.85; k = 1.15.

Here the prime denotes the cross section ahead of the shock, while the double prime denotes the section after the shock.

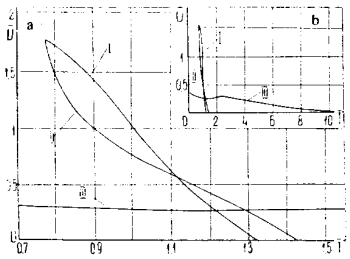

Fig. 4. Volt-ampere characteristics for regimes I, II, and III for S = 0.75. Figures 4a, b differ in the scales chosen for the coordinate axes.

Having integrated system (6)–(8) with the initial conditions (10) and having utilized conditions (14) to relate the parameters ahead of and beyond the shock, we find the distribution of the Mach number M over the length of the channel for an arbitrary value of the shock coordinate.

The distribution curves for the current $\bar{I} = 0.7$ are shown in Fig. 2b. The Mach number, diminishing over the channel length when $M > 1$, becomes subsonic behind the compression shock, and then increases until thermodynamic blockage sets in. It is interesting to note that, unlike flow in tubes with friction [5], the maximum channel length corresponding to the speed of sound at the outlet is greater for shockfree flow than the maximum length in the presence of a shock within the channel. This length is at its minimum when the shock is positioned at the channel inlet and increases monotonically as the shock coordinate increases. Hence, first, flow with a shock in the MHD channel (regime II) cannot—as the flow without shocks (regime I) cannot—be attained with currents smaller than $\bar{I}_\alpha$. Second, as follows from Fig. 2b, given the identical current and a specified channel length, both regime I and regime II are possible in principle. In regime I we have $M > 1$ at the outlet, while in regime II we have $M = 1$. The pressure at the outlet from the channel in regime II is greater than the counterpressure of the medium. Consequently, at the channel outlet in regime II condition $M = 1$ must be satisfied, rather than condition $M < 1$; $p = p'$.

For each value of the current and for the specified length S we can find a position for the shock in the channel so that the condition $M = 1$ is maintained at the outlet. In this way we establish the unique relationship—corresponding to this regime—between the current and the voltage, i.e., we can plot the volt-ampere characteristics for the flow regimes with a shock in the channel. Figure 4 shows the volt-ampere characteristic for a flow regime with a shock in the channel when $S = 0.75$; $\beta_{i0} = 5$; $\eta_{el0} = 0.85$; $k = 1.115$; $M_{01} = 2.2$.

The shock coordinate $\bar{x}$ in this case ranges between 0.75 and 0.55, with its value at the minimum when $\bar{I} = 1$.

§ 3b. Let us examine the possibility of flow regimes existing with a normal compression shock in the Laval nozzle (regime III).

Assuming that the shock in the nozzle occurs when $M = M'_{sh}$, we find the dimensionless parameters ahead of the compression shock and the dimensionless area of the lateral cross section:

$$\tau' = [1 + (k-1)2^{-1}M_{01}^2][1 + (k-1)2^{-1}M'^2_{sh}]^{-1},$$

$$\bar{v}' = M'_{sh}M_{01}^{-1}[1 + {}^1/_2(k-1)M_{01}^2]^{1/2} \times \times [1 + {}^1/_2(k-1)M'^2_{sh}]^{-1/2}; \quad (15)$$

$$\bar{F}' = M'_{sh}M_{01}^{-1}\{[1 + {}^1/_2(k-1)M_{01}^2] \times \times [1 + {}^1/_2(k-1)M'^2_{sh}]^{-1}\}^{(k+1)/2(k-1)}. \quad (16)$$

Further, using (14), we calculate the thermodynamic quantities beyond the compression shock and with formulas (15) (after first having replaced M_{01} with M''_{sh} and M'_{sh} with M_1 in them), we find the thermodynamic quantities $\bar{v}_1$ and τ_1 at the channel inlet. Here M_1 is determined from the condition $\bar{F}_1 = 1$.

The change in the Mach number M along the channel in regime III for various values of M_{sh} is shown in Fig. 2b. The flow is subsonic over the entire length of the channel. The Mach number M increases over the channel length until thermodynamic blockage sets in. The pressure at the channel outlet is always higher in this case than the counterpressure of the medium, which coincides with the pressure at the outlet in the nominal regime. Consequently, in analogy with the situation for regime II, it is possible to have a flow with a shock in the nozzle when we have the condition $M = 1$ at the outlet. The volt-ampere characteristic for $S = 0.75$ which corresponds to regime III is shown in Fig. 4. The quantity M_{sh} in this case assumes values of 2–2.1, depending on the current.

We note that in the case under consideration, for large currents ($\bar{I} \sim 7$) and low voltages, i.e., for small load resistances, we observe tunneling through the speed of sound from $M < 1$ to $M > 1$ (regime IIIa). That segment of the channel where this transition occurred was consuming electric power, although the channel as a whole could continue to work, as before, in the generator regime. The possibility of this type of tunnel transition has been demonstrated in [6].

As we can see from Fig. 2b, with an MHD interaction parameter smaller than some limit (the position of the shock at the inlet corresponds to this value of S, subsequently denoted as S_α) only regime I is possible. When $S = S_\alpha$, it is possible to have the regime in which there is a shock at the inlet to the channel, i.e., regimes II and III coincide. Finally, when $S > S_\alpha$ we can construct $M(S\bar{x})$ for all regimes.

For large values of S the generator must function strictly in the theoretical regime, since with even a slight deviation of the current from the nominal value there will be blockage in regime I, and regime III (with a shock in the nozzle) will become the only one possible.

The above-cited volt-ampere characteristics should be compared with the experimental characteristics.

However, existing experimental results [7, 8] have been obtained on installations of comparatively small scale, where the effect of the walls (friction, heat transfer, and most importantly, the electrode potential drops) may be substantial. It is demonstrated below that the results of calculations using a one-dimensional model considering friction, heat transfer, and the electrode drop can be close to the experimental results [7], given specific assumptions as to the relationship between the electrode potential drop and the current density. The computational system of equations coincides with (1), except that the force of friction $\xi\rho v^2/2D$, the heat flux $q\Pi/F$ per unit channel length, and the electrode potential drop Δ have been introduced into the equations: $E_y - E_x/\gamma = \Delta/b$, where b is the width of the channel.

The heat flow q (the sum of the convective and radiative flows) was calculated on the basis of the usual formulas for a long channel.

We have used the following initial data [7]:

$$p^* = 3 \text{ at}, B = 2 \text{ tesla}, \sigma_1 = 19 \text{ mho/m},$$

$$F = 0.102 \text{ m}^2; \times 0.051 \text{ m}^2, v = 1700 \text{ m/sec}.$$

The angle of channel divergence is 2.4°; the length is 0.9 m. From the table in [9] we have the found that

$$p_1 = 0.75 \text{ at}; \; T_1 = 2880° \text{ K};$$
$$c_p/c_v = 1.1; \; gR = 330; \; \lambda_1 = 1.6.$$

Here λ_1 is the velocity factor.

The electrode drop as a function of current density is taken as $\Delta = \Delta_1 + kj_y$, where Δ_1 = 80 V, k = 0.21 $m^2 \cdot$ ohm. The assumed magnitude of Δ_1 corresponds to the repeatedly observed "threshold" voltage of cold metal electrodes, while the quantity k is the only empirical parameter which brings the calculation with simple equations into approximate agreement with experiment over the entire volt-ampere characteristic from the standing current to the short-circuit current.

REFERENCES

1. A. Montardi, collection: MHD Generators of Electrical Energy [in Russian], VINITI, 1963.

2. V. I. Kovbasyuk and S. A. Medin, in: Electricity from MHD, Vienna, IAEA, **1**, 431, 1966.

3. A. I. El'kin, Magnitnaya Gidrodinamika [Magnetohydrodynamics], 3, 91, 1967.

4. A. I. El'kin and E. I. Yantovskii, Izv. AN SSSR, Energetika i transport, 6, 107, 1967.

5. Collection: Fundamentals of Gasdynamics, **3**, series: The Aerodynamics of High Velocities and Jet Engineering [Russian translation], IL, Moscow, 1963.

6. L. A. Vulis and M. K. Kusainov, Teplofizika vysokikh temperatur, 4, 662, 1967.

7. J. B. Dicks, V. C. L. Vu, D. Denzel, S. Witkowski, R. V. Shanklin, and V. Litzow, Symp. MHD electrical power generation, Warsaw, 24–30 July 1968, SM-107/28.

8. J. Teno, T. R. Brogan, and Z. R. Dincenno, Electricity from MHD, 3, Proc. of a Symp., Salzburg, 4–8 July 1966.

9. L. K. Garkusha and G. M. Shchegolev, Entropy Diagrams of Combustion Products (to 4000° K) [in Russian], Naukova dumka, Kiev, 1968.

24 July 1968